Chapter III

Preliminary drop-tower experiments on liquid-interface geometry in partially filled containers at zero gravity.

(In Experiments in Fluids **8**, *312-318(1990))*

G. Smedley
Graduate Aeronautical Laboratory
California Institute of Technology
Mail code: 205-45
Pasadena, CA 91125
U.S.A.

Abstract

Plexiglas containers with rounded trapezoidal cross sections were designed and built to test the validity of Concus and Finn's existence theorem (1974,1983) for a bounded free liquid surface at zero gravity. Experiments were carried out at the NASA Lewis two-second drop tower. Dyed ethanol-water solutions and three immiscible liquid pairs, with one liquid dyed, were tested. High-speed movies were used to record the liquid motion. Liquid rose to the top of the smaller end of the containers when the contact angle was small enough, in agreement with the theory. Liquid interface motion demonstrated a strong dependence on physical properties, including surface roughness and contamination.

1 Introduction

For a partially filled container in a zero-gravity environment, the location of the liquid is not known a priori. This fact poses several practical problems in areas such as the management of spacecraft fuel and the use of multi-phase heat pipes. Concus and Finn (1974) and Finn (1983) developed a theorem that addresses the static problem of existence for a bounded liquid free surface at zero gravity in a cylinder of arbitrary cross section. Given the geometry of the container and the contact angle between the liquid and solid, the theory, outlined in section 2 below, predicts whether the equilibrium shape of the liquid free surface at zero gravity is bounded or goes to infinity. Because the behavior of moving contact lines is not understood, the solution of the corresponding dynamic problem is still far beyond the reach of theory and numerical computation. Nevertheless, a valid static theory can be very useful for design of a dynamic experiment. If the liquid moves as the static theory suggests it should, confidence in use of the theory to design containers for measurement of dynamic surface behavior would be increased. To test the static theory in this sense, several experiments were carried out in the NASA Lewis two-second drop tower. Six mixtures of ethanol and water under air, and three immiscible liquid pairs, were dropped in plexiglas containers designed according to the static theory. The experiments are described in sections 3 and 4.

2 Theory

The following description of the theory is a general outline of the theory presented in Finn (1983); a more detailed analytical and numerical application of this theory to several different cylinder cross-sections will be reported in another paper. A standard variational technique is used to minimize an expression for the free energy of a liquid in a container at zero gravity (Fig. 1). The free energy includes the free surface energy ($E_S = \sigma S$) and the wetting energy ($E_{S^*} = -\lambda_0 \sigma S^*$), where σ is the surface tension, S and S^* are the free surface area and the wetted surface area, respectively, and λ_0 is a constant of proportionality. The total volume of the liquid is held constant as a constraint ($\lambda_1 V$). Thus

$$E(S) = S - \lambda_0 S^* + \frac{\lambda_1}{\sigma} V \tag{1}$$

Minimization of the free energy (Eq. 1) yields the Laplace-Young equation for a static liquid free surface in a cylinder of arbitrary cross section at zero gravity;

$$\text{div } \mathbf{T}(h) = \frac{\Sigma \cos\gamma}{\Omega} \tag{2a}$$

$$\nu \cdot \mathbf{T}(h) = \cos\gamma = \lambda_0 \tag{2b}$$

where ν is the unit outward normal, Σ and Ω are the perimeter and area of the cross section; γ is the contact angle, measured in the liquid; $h = h(x,y)$ is the height of the free surface; and

$$\mathbf{T}(h) = \frac{\nabla h}{(1 + |\nabla h|^2)^{1/2}} \tag{2c}$$

Consider a cross section of the container, normal to the axis (Fig. 2). The free surface intersects the cross section along a curve Γ. Integration of equation (2a) over this section yields an energy per unit length (Eq. 3), which is a two-dimensional analog to the three-dimensional energy (Eq. 1). There is a close analogy between the free surface area (S), the wetted surface area (S^*), and the liquid volume (V) in equation (1) and the length of the curve (Γ), the length of the wetted boundary (Σ^*), and the liquid area (Ω^*) in equation (3).

$$\Phi(\Gamma) = \Gamma - (\cos\gamma)\Sigma^* + \left[\frac{\Sigma \cos\gamma}{\Omega}\right] \Omega^* \tag{3}$$

If $\Phi \leq 0$, the free surface appears in the cross section. Thus a configuration of minimum energy requires the presence of liquid between the container wall and the convex side of the curve Γ. Minimization of equation (3) shows that Γ is a circular arc of radius $R_\gamma = \frac{\Omega}{\Sigma \cos\gamma}$. If $\Phi > 0$, however, the free surface does not appear in the cross section. Therefore, the functional Φ enables us to characterize the expected equilibrium interface in a particular geometry at zero gravity.

The theory predicts that liquid rises to infinity on some part of the wall of a two-dimensional container if $\Phi \leq 0$. However, the theory does not indicate how high the liquid will rise, if at all, for $\Phi > 0$. To determine the height of the equilibrium free surface, in this case, it is necessary to solve the static problem (2) for the specific cylinder of interest. Such a solution h(x,y) is available for a particular rounded trapezoid (Bainton, 1986). The shape was chosen, using the static theory, to have a critical contact angle of 30°. Free-surface solutions along the longer axis of symmetry of the cross section are shown in Fig. 3 for $\gamma = 30.6°$, 40°, 50°, and 80°. The difference between the maximum and minimum of each curve is extracted as a function of γ in Fig. 4. No solution was possible for $\gamma \leq 30°$, as predicted by the theory. The Newton's method used for these calculations did not converge for $\gamma < 30.6°$. There is a smooth but rapid trend in the rise of the liquid toward infinity as the predicted critical contact angle is approached.

3 Experiment

A cylindrical container with rounded trapezoid cross section was designed using the same geometry considered by Bainton (Fig. 5). The functional Φ (Eq. 3) depends only on the parameters α, β, and γ, where $\alpha \leq 90°$ is the half angle of the extended sides, $0 \leq \beta \leq 1$ is the ratio of the radii, and γ is the contact angle. One geometry can therefore be used to exhibit behavior for both $\Phi > 0$ and $\Phi \leq 0$ by changing the liquid, thereby changing γ. For a liquid with $\gamma > \gamma_{crit}$ (supercritical), $\Phi > 0$, and the liquid is expected to rise to a finite height in the narrow end of the container at zero gravity (Fig. 4). For $\gamma \leq \gamma_{crit}$ (subcritical), $\Phi \leq 0$. According to Concus and Finn's static theory, the liquid is expected to rise to an infinite height (Fig. 4). In a container of finite height, the top of the container (Fig. 4) interferes with the theoretical behavior. Numerically computed heights greater than 6.25 cannot be discerned from infinite heights with the containers used in this work.

Three containers were machined from solid blocks of plexiglas using a computer-controlled milling machine with an accuracy of 0.0002" and a repeatability of 0.0005". The nominal dimensions of the plexiglas containers are shown in Fig. 6. Two of the containers were designed for $\Phi = 0$ at $\gamma = 30°$ (the critical contact angle). One of these (A) was polished using

1000-grit grinding polish, the other (B) was polished using 400-grit. The third container (C) was inadvertently cut oversize with larger radii and was left unpolished, with $\gamma_{crit} \approx 28°$. This container provided some data regarding the effect of roughness on the predictions of the static theory.

The liquids that were used in the experiments fell into two groups. The first group consisted of mixtures, in various proportions, of ethanol and water under air. This group allowed us to vary the contact angle by varying the concentration of ethanol (0% to 50% in steps of 10%) and thus to determine whether the static theory correctly predicted the critical contact angle for the geometry in question. The second group of liquids consisted of three immiscible liquid pairs, intended to show the effects of liquid properties, particularly viscosity, on the time scale of the liquid motion at zero gravity. Since the dominant factors determining this time scale are not known, the three liquid pairs were chosen to have very different physical properties to cover a wide range of behavior (Table 1). The three pairs were: (1) glycerol tributanoate over ethylene glycol, (2) diethyl diethyl malonate over formamide, and (3) 1-chlorohexane over formamide. Liquid pairs 1 and 2 were chosen because both had subcritical contact angles with PMMA and pair 1 was three to five times more viscous than pair 2. Pair 3 was chosen because of its supercritical contact angle. In addition, liquid pairs have the advantage that the difference in index of refraction of the liquids is small. The total internal reflection that results from a lack of index match between the gas and the liquid in the ethanol-water samples causes the interface to appear as a dark band (Fig. 7a-7g), thereby preventing accurate measurement of its position as a surface in two dimensions.

The experiments were carried out in the two-second drop tower at NASA Lewis Research Center. Before each drop, the containers were cleaned in an ultrasonic bath of Freon 113 (1,2,2-trifloro-1,1,2-trichloroethane) for about five minutes and allowed to air dry. They were filled approximately one-third full (20ml) with various mixtures of ethanol and water containing a small amount of blue vegetable dye. The container lids were sealed quickly to prevent evaporative loss of ethanol, which would reduce the ethanol concentration. The vapor/liquid system was then allowed to come to equilibrium before the drop. Complete filling of containers with immiscible liquid pairs was achieved by assembling them while fully submerged. In all

cases, the upper liquid was expected to move down the narrow end of the container because the smaller contact angle existed between the upper liquid and the container walls. It was therefore necessary to have the container approximately one-third full of the upper liquid and two-thirds full of the lower one (Fig. 7h). Dying of the lower liquid was easily achieved, using a blue vegetable dye that was not soluble in the upper liquid.

High-speed movies were taken with a 1962 D. B. Milikan camera (DBM 4) set to run at 400 frames per second. The camera was focused on the long side of the containers with the narrow end of the rounded trapezoid cross section on the left. Back lighting of the containers and liquids was provided by a diffuse back-lighted screen. A digital clock display, stated to be accurate to 0.001 seconds, was also mounted on the test rig and was recorded on the film.

4 Results

The instrumentation supplied for the drop-tower tests was not always adequate. This fact together with limited time at the facility prevented a full evaluation of the many experimental questions posed in the preceding sections. As a result, the data obtained represent an incomplete set. In the following discussion, the results obtained for 50% ethanol and for liquid pair 1 are emphasized, while the results from the rest of the liquids are briefly mentioned.

Quantitative measurements from the high-speed films required a knowledge of the actual framing rate of the camera. The first decision to be made was whether to trust the camera setting (400 fps) or the digital clock, since these did not agree. The camera was started and allowed to accelerate for two seconds prior to the drop, and the clock was started at the instant the experimental package was released. Provided that the batteries were in good condition, it was probably safe to assume that the camera ran at the same equilibrium speed for the full duration of the two-second drop. Except for the first test, the batteries in the test rig were new and nearly fully charged, so that the voltage should not have varied much throughout the drop duration. With this assumption, the clock readout was accepted as accurate, provided that it could be deciphered. The clock did not hold numbers on its four-digit display until they changed; instead each of the four numbers was turned on and off in sequence whether it had changed or not. The clock readout looked reasonable to the unaided eye, but to the high speed

camera only one or two digits were visible during a single frame. During the worst asynchrony of clock and camera, particular clock digits would not be seen for four or five consecutive frames. Although the clock read out to 0.001 second, the accuracy of determining the frame time was not better than 0.005 second. To determine the framing rate of the camera, film frames were counted while using the clock as a time reference. The film speed was found to be fairly constant (278 fps ± 2%) for the 50% ethanol case, but differed from the specified 400 fps by 30%. This measured framing rate was used to interpolate the elapsed time for a given film frame.

The experiments involved the use of three containers. The results are very scattered and exhibit a wide range of behavior. Still photographs taken from the high-speed films are shown in Figs. 7a-7h. The dimensions of the liquid/vapor containment area shown in these figures are approximately 2.5" by 2.5" (Fig. 6). Water (0% ethanol) in container A and 10% ethanol in container C were the only liquid mixtures that reached equilibrium and did not reach the roof of the containers (Fig. 7a,7b). The 10% ethanol mixture started its rise very erratically, with many notches in the contact line and waves on the surface (Fig 7b). These effects were probably caused by jerky movement of the contact line due to the roughness of the container walls. The experiment involving 20% ethanol in container A was very inconclusive. Waves were observed on the surface of the liquid throughout the entire drop and the liquid did not rise (Fig. 7c), perhaps indicating that the drop package was bumped as it was dropped. Neither 30% ethanol in container C nor 40% ethanol in container B (Fig. 7d, 7f) achieved equilibrium during the two seconds of drop time. The liquid in container C exhibited the same notched contact line that moved erratically up the walls of the container as in the 10%-ethanol case. The 40% ethanol moved up the polished walls of container B very smoothly. Measurements were made from projected film images of the liquid rise (Fig. 8a). Qualitatively, the results obtained compare quite well with the results obtained for 50% ethanol in the same container (Fig. 8b). There was one notable difference between the two cases; the 40% ethanol contact line moved approximately 20% slower (average ≈ 3.07 cm/sec) up the left side and 30% slower (≈ 1.41 cm/sec) across the roof than the 50% ethanol contact line (Fig. 8a, 8b). One or both of these discrepancies may be caused by some type of contamination that increased the contact angle (compare photos 7e-7g), thereby slowing the progress of the contact line. This

observation indicates that the contact angle is an important contributor to the velocity of the contact line at zero gravity; the larger the angle, the slower the motion, despite the fact that the surface tension is higher.

Figure 7g shows a sequence of frames from a high-speed movie of the experiment using a mixture of equal parts by volume of water and ethanol under air, for which the contact angle on plexiglas is about 23°. The smaller radius is at the left, and the two dashed lines in the initial frame are the projection of the critical arc Γ for this geometry. When the body force due to gravity is first removed, and again when the rising liquid at the left first reaches the top of the container, rapid dynamic movement of the contact line is manifested mainly by necking; i.e., by withdrawal of liquid from the near vicinity of the contact region rather than from the distant bulk of the liquid. Note also that the contact line at the right is advancing during the first half of the experiment and receding during the second half, with some visual evidence of a dependence of contact angle on the direction of the velocity.

Measurements of liquid interface positions for 50% ethanol in container B were made directly from projected film images and non-dimensionalized with the larger radius of the container cross section. The results are shown in Fig. 8b. The measurements include the height of the free-surface minimum, the height of the right and left contact lines, and the distance traveled across the top of the container. Note that initially the liquid moves very quickly at both ends at about the same rate and the minimum decreases at a comparable rate, as the interface moves from a nominally plane configuration toward one of much higher curvature. The presence of free-surface motion during the first half-second of the drop, indicated by the initial necking down, is accompanied by oscillation in the height of the surface minimum. The advance and retreat of the right contact line are easily seen. Note that the retreat of the right contact line and the reduction in the surface minimum occur at fairly constant rates after approximately one second. When the left contact line reaches the top of the container, the velocity of retreat of the right contact line and the minimum of the free surface change; the surface minimum decreases more quickly and the right contact line height recedes more slowly. This behavior seems to indicate a withdrawal of liquid from the bulk rather than from the vicinity of the contact line, contrary to the condition that existed during the earlier part of the

drop. Also notice that as the left contact line climbs, its velocity decreases (average $\approx$ 3.87 cm/sec). Upon reaching the top, experimental error caused by lack of index match across the interface introduces an artificial jump in the contact-line position. The liquid then proceeds across the top of the container at a nearly constant rate ($\approx$ 2.04 cm/sec). Given more time, we might have been able to see the bottom of the container become uncovered, since the surface minimum can be extrapolated to zero after roughly another two seconds.

The three experiments involving liquid pairs exhibited similar behavior on a much longer time scale. The interface moved very slowly in all three cases. The final state for pair 1 is shown in Fig. 7h. Corresponding figures for pairs 2 and 3 are not given since their final appearance is very similar to Fig. 7h. It was not possible to determine the difference between supercritical and subcritical behavior with only two seconds of zero gravity. Evidence for differences in time scale is provided by differences in the advancing velocity of the left contact line (Table 1). Interfacial tensions and contact angles were found by Smedley and Coles (1989). Note that the pair 1, with the smallest contact angle, had the highest contact-line velocity despite the fact that it was the most viscous, again indicating the importance of contact angle in determining contact-line velocity. A careful study of the table suggests that the relative magnitudes of the contact line velocities are determined by the product of the surface tension and the cosine of the contact angle. The data also seem to indicate a dependence on the degree of criticality of the contact angle; subcritical angles yield higher contact-line velocities than supercritical angles for similar values of $\sigma\cos\gamma$ (compare pair 1 and pair 3 in table 1). Also, pair 1, which has a more subcritical contact angle than pair 2, moves at a rate three times higher than pair 2 despite their similar interfacial tensions. The interfaces of the liquid pairs advanced at the following average rates: pair 1 $\approx$ 0.28 cm/sec, pair 2 $\approx$ 0.09 cm/sec, pair 3 $\approx$ 0.13 cm/sec. These velocities of advance were nearly constant over the entire duration of the drop. The results depicted in Fig. 8c for pair 1 are typical for these three liquid pairs.

The measured liquid interface positions for liquid pair (1) (Fig. 8c) changed much less dramatically than those for 50% ethanol. The interface moves from the top down, and measurements are given as distances from the top of the container. This liquid pair reacts much more slowly to the sudden removal of the gravitational body force. A region of very quick

motion does not exist near the beginning of the drop; however, some necking is still indicated by the photographs and by the behavior of the minimum height of the interface. The oscillation in the surface minimum of this liquid pair is smaller by about a factor of two than the corresponding one for 50% ethanol. The left and right contact lines advance at monotonic rates that are similar in magnitude, with the left contact line moving slightly faster. According to the measurements of contact angle, this particular liquid pair was subcritical; therefore, the liquid interface should go to infinity or to the bottom of the container (Fig. 7h). But, since the interface minimum was moving approximately seven times slower than for 50% ethanol, and had farther to go, it would not have reached the bottom until roughly another sixteen seconds had elapsed.

5 Discussion and Conclusions

All nine of the experiments discussed above are compared to the theory in Fig. 4. As previously mentioned, at the end of section 2 and the beginning of section 3, Fig. 4 contains the theoretical and numerical results for the case $\gamma_{crit} = 30°$. This plot also contains symbols representing the difference between the measured maximum and minimum heights of the final state, of each liquid surface or interface, of the nine experiments reported here. The heights are nondimensionalized with the large radius of the cross section and plotted against the measured contact angle.

The symbols labeled 1 through 6 are the results for the various ethanol solutions 0%(10%)50% respectively. The symbols labeled 7 through 9 are the results for liquid pairs 1 through 3 respectively. Consider first the ethanol solutions compared to the dotted numerical curve. There is a substantial scatter; however, the trend is correct: as the contact angle decreases toward the critical value (30°), the liquid rises to greater heights. Some scatter can be attributed to the fact that contact angles were measured in the lab rather than on-site, since appropriate equipment for these measurements was not available on-site. In the lab, contact angles for the ethanol and water solutions were measured for a sessile drop on plexiglas using a cathetometer. Contact angles for the three immiscible liquid pairs were measured against a blade of plexiglas inserted into a test tube containing the liquid pair (Smedley and Coles, 1989).

The 30%, 40%, and 50% ethanol solutions (symbols 4, 5, and 6) all reached the roof of their containers (Fig. 7d, 7f, and 7g). The upper limits of the containers are shown as dashed lines on the plot (Fig. 4). The symbols 5 and 6, however, are not located on the upper dashed line, since the plotted height is the difference between the maximum and minimum of the liquid surface. A symbol would only rest on the dashed line if the bottom of the container was bare of liquid. If less liquid had been used in these cases, this may have happened. Limited time at the facility did not allow this adjustment of the experiment to be made. The same is true for symbol 4 (30% ethanol), which does not lie on the lower dashed line. Symbol 3 (20% ethanol) represents the case that may have been bumped and therefore never realized zero gravity (see section 4). Symbol 2 (10% ethanol) is a large distance from the numerical results. This might be accounted for by an error in the contact angle, measured in the lab rather than site, and/or by the roughness of the wall perhaps wicking the liquid to a higher than expected height. The location of symbol 1 (0% ethanol) is reasonably close to the numerical results.

The final rise heights for the three liquid pairs (symbols 7, 8, and 9) were small compared to the results for the ethanol solutions. Note that the upper dashed line represents the bottom of the container when considering the three liquid pairs, since the upper liquid moved down toward the bottom of the container (see section 3). Despite the fact that pairs 1 and 2 (symbols 7 and 8) had sub-critical contact angles, symbols 7 and 8 did not come close to the bottom of the container. These pairs did not reach equilibrium in the two seconds of zero gravity. The velocities of the moving interfaces were too slow (Table 1). Symbol 9 (liquid pair 3) is reasonably close to the numerical curve despite the fact that it also had not reached equilibrium in two seconds.

The theory, combined with numerical solutions, appears to be an adequate tool for the design of containers that incorporate strong dynamic free-surface behavior when zero gravity is suddenly imposed. This fact provides support for the use of the static theory as a means to design containers to study dynamic free surface behavior at zero gravity. The dynamic behavior of liquid interfaces demonstrates strong dependence on physical properties. However, the data presented here do not represent a large enough range to support conclusive statements regarding this dependence. Observations suggest that the dynamics of a liquid free surface or interface do

not depend on the contact angle and physical properties in a simple manner. Wall roughness appears to cause a notched, erratic motion of the contact line, whereas smooth walls lead to very smooth motion. Equilibrium states for liquid pairs were not attainable in two seconds of zero gravity. Further work is needed to determine dynamic time constants based on the physical properties of single liquids or liquid pairs.

This material is based upon work supported by the U.S. National Aeronautics and Space Administration and the University of California. The opinions, findings, conclusions and recommendations are those of the authors and not necessarily of the U.S. National Aeronautics and Space Administration or the University of California.

References

Bainton,M.C. 1986: Fluid interfaces in the absence of gravity (Masters Thesis). Lawr. Berk. Lab. U. of CA; Dept. of Math.

Concus,P. and Finn,R. 1974: On capillary free surfaces in the absence of gravity. Acta. Math., 132,177-198.

Finn,R. 1983: Existence criteria for capillary free surfaces without gravity. Ind. Univ. Math. J. 32(3), 439-460.

Smedley,G. and Coles,D. 1989: Some immiscible liquid pairs. Submitted to the Journal of Colloid and Interface Science.

Figure Captions

Figure 1: Generic cylinder partially filled with liquid.

Figure 2: Cross section of generic cylinder.

Figure 3: Computed equilibrium free surfaces for $\gamma = 30.6°, 40°, 50°$, and $80°$.

Figure 4: Liquid height (max - min) in rounded trapezoid. Symbols: (1)-(6) ethanol and water mixtures tabulated below, (7) glycerol tributanoate over ethylene glycol, (8) diethyl diethyl malonate over formamide, (9) 1-chlorohexane over formamide.

Symbol #	1	2	3	4	5	6	7	8	9
Container	A	C	A	C	B	B	A	B	B
Ethanol %	0	10	20	30	40	50	--	--	--

Figure 5: Rounded trapezoid cross section.

α = half angle of extended sides.

$\beta = \frac{b}{a}$ = radius parameter.

Figure 6: Nominal dimensions of constructed containers.

Containers A and B: $\alpha \approx 6.16°$; $\beta = \frac{0.2''}{0.4''} = 0.5$; $\gamma_{crit} = 30°$.

Container C: $\alpha \approx 6.73°$; $\beta = \frac{0.22''}{0.44''} = 0.5$; $\gamma_{crit} \approx 28°$.

Figure 7a: Water (0% ethanol) in container A at final time.

Figure 7b: 10% ethanol solution in container C at final time.

Figure 7c: 20% ethanol solution in container A at final time.

Figure 7d: 30% ethanol solution in container C at final time.

Figure 7e: 40% ethanol solution in container B at T = 0.5 seconds.

Figure 7f: 40% ethanol solution in container B at final time.

Figure 7g: 50% ethanol solution in container A at times shown.

Figure 7h: Glycerol tributanoate over ethylene glycol in container A at final time.

Figure 8a: Position of free surface of 40% ethanol solution at zero gravity.

Figure 8b: Position of free surface of 50% ethanol solution at zero gravity.

Figure 8c: Position of interface of glycerol tributanoate over ethylene glycol at zero gravity.

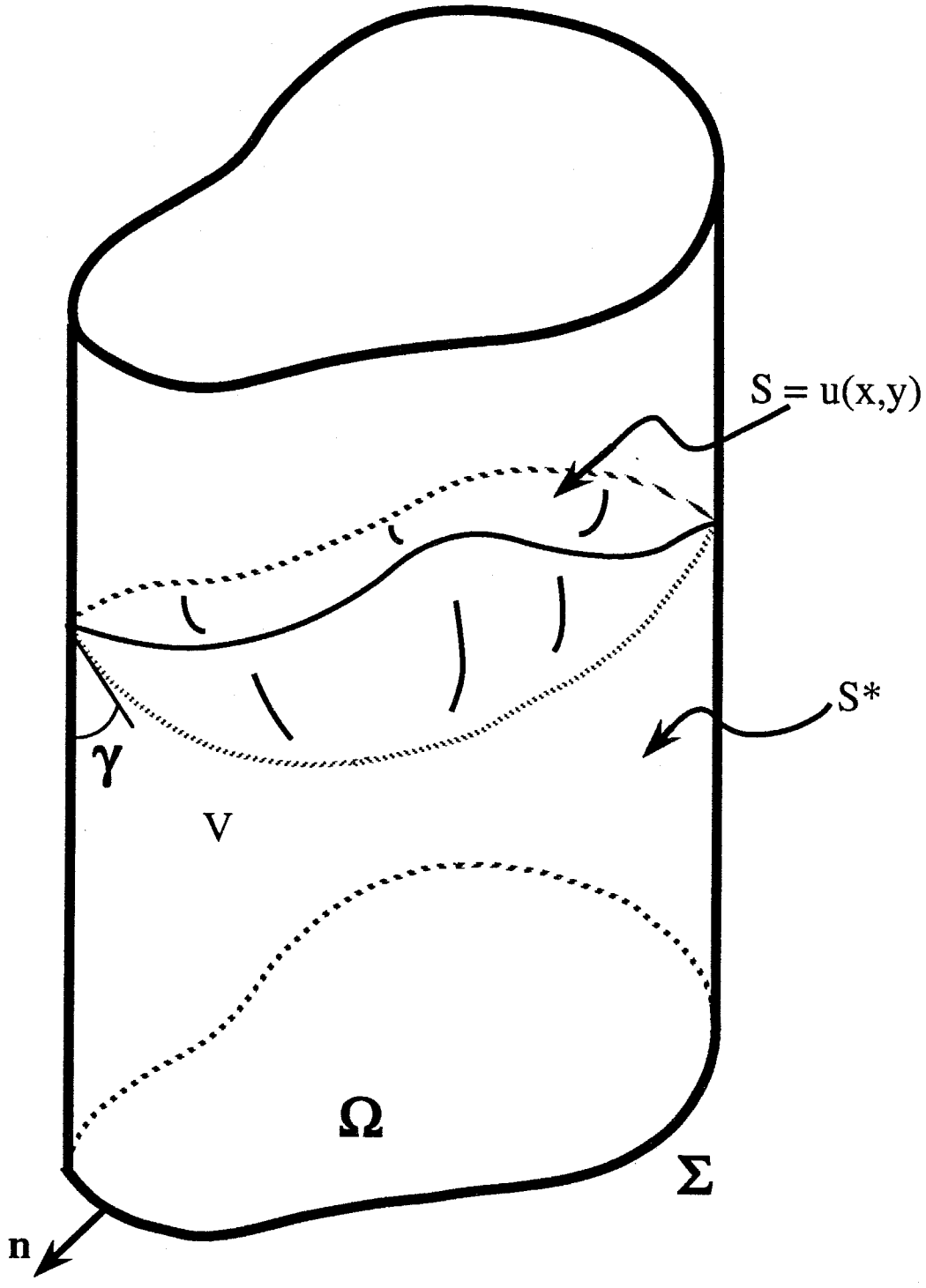

Figure 1 Generic cylinder partially filled with liquid

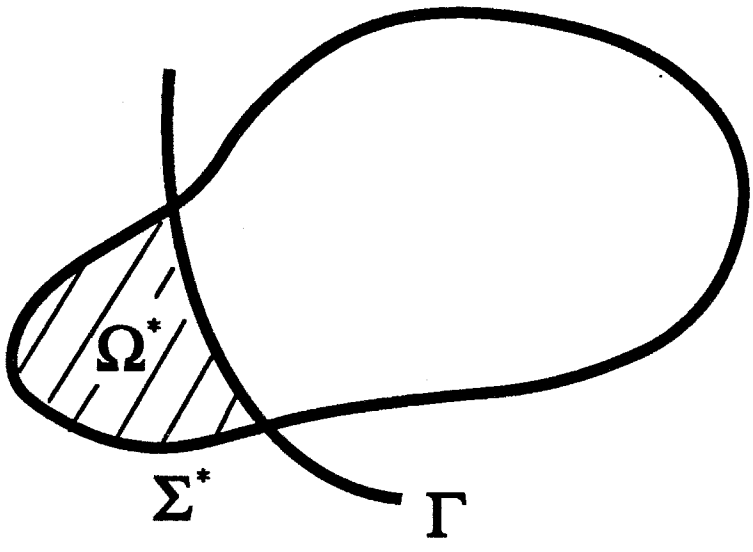

Figure 2 Cross section of generic cylinder

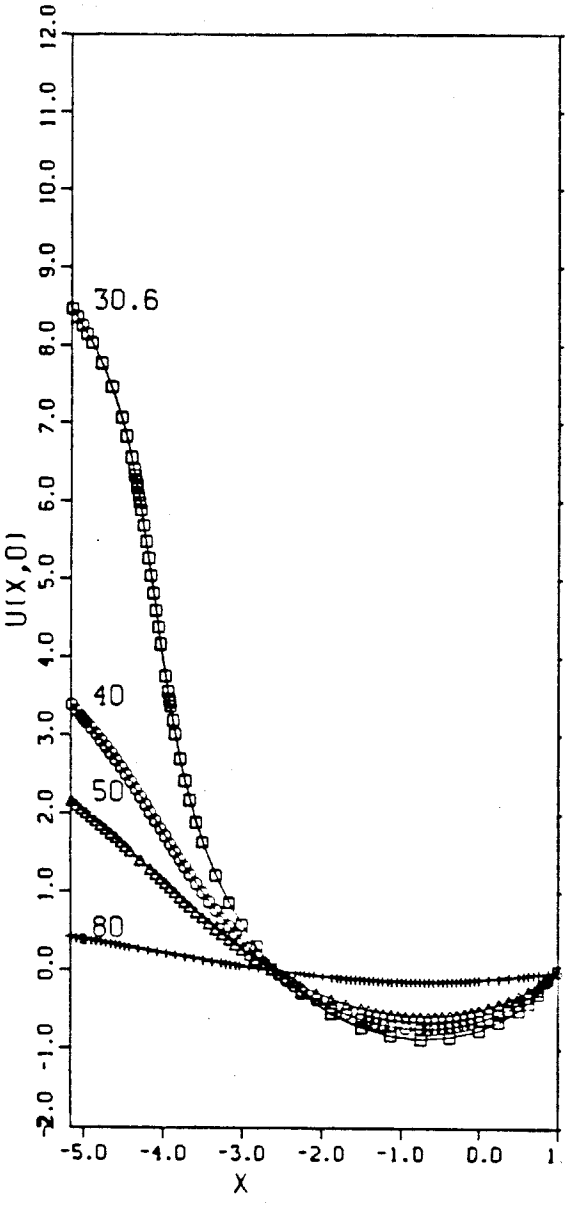
U(X,0)
X
30.6
40
50
80
12.0
11.0
10.0
9.0
8.0
7.0
6.0
5.0
4.0
3.0
2.0
1.0
0.0
-1.0
-2.0
-5.0
-4.0
-3.0
-2.0
-1.0
0.0

Figure 3

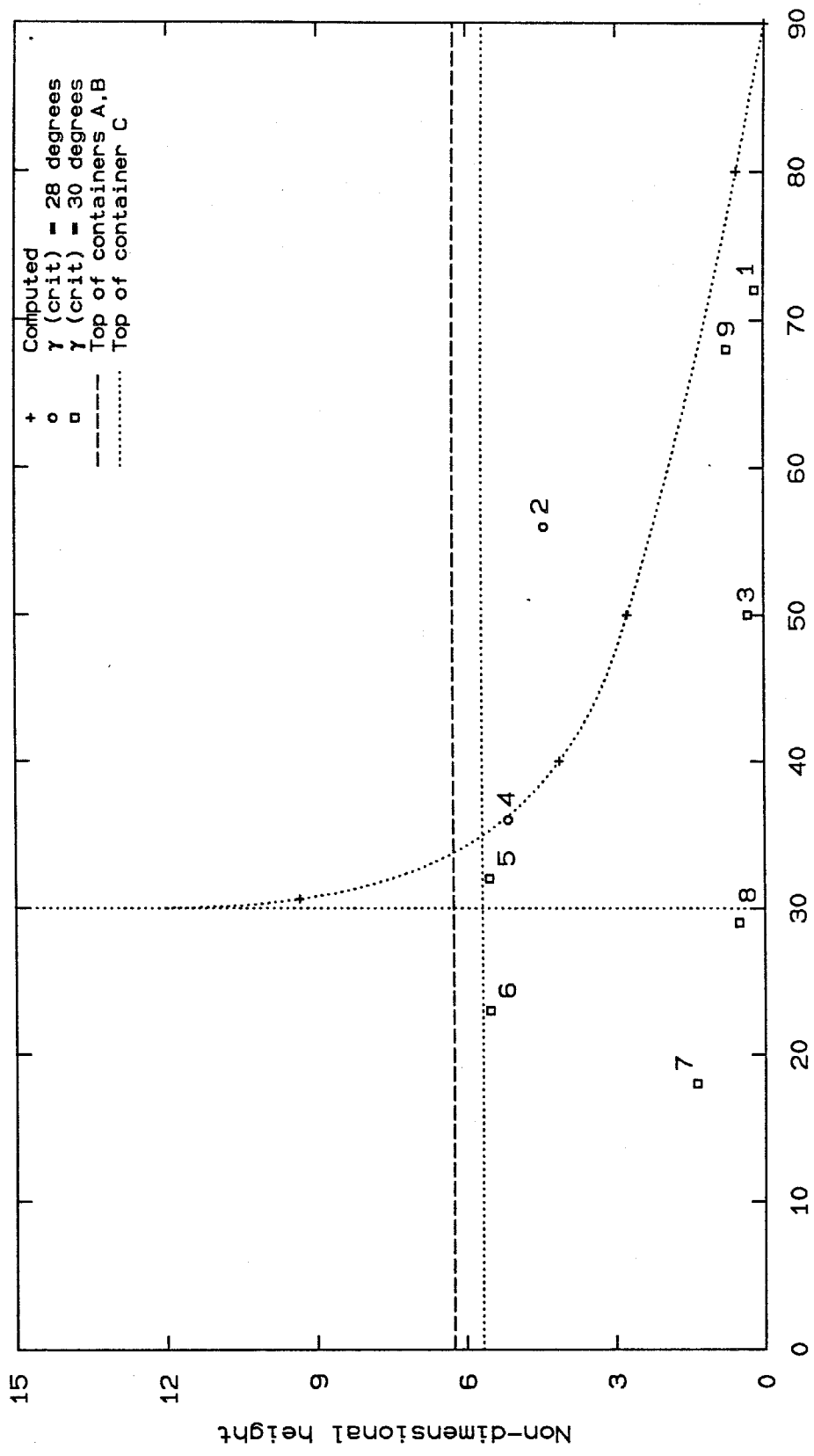

Figure 4 See figure caption

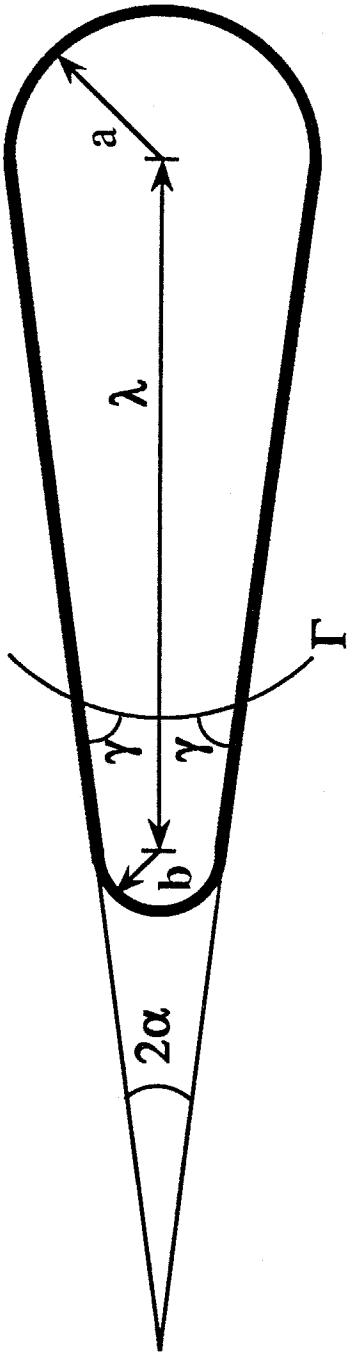

α = half angle of extended sides
β = b/a = radius parameter

Figure 5 Rounded trapezoid cross section

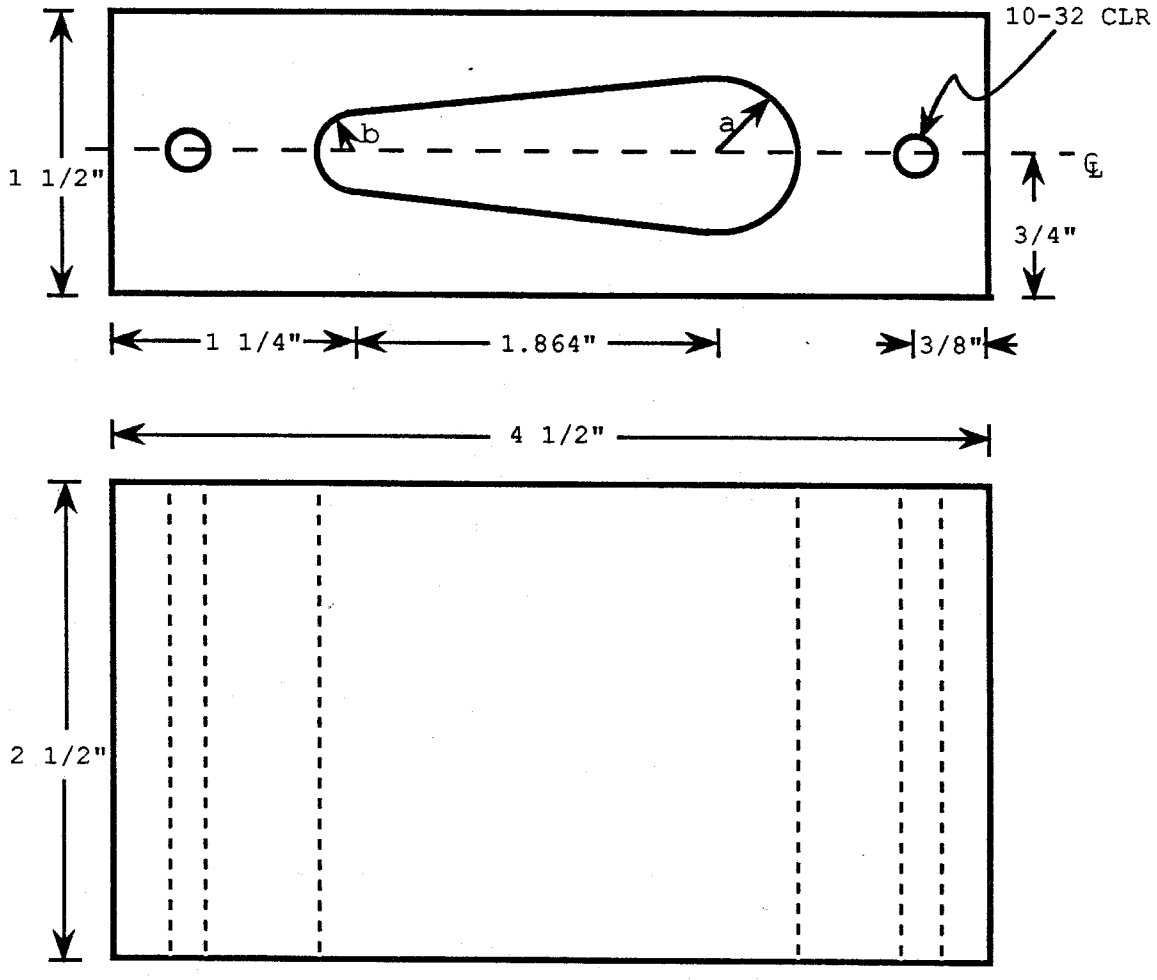

Containers A and B: $\alpha \cong 6.16$ degrees; $\beta = 0.2"/0.4" = 0.5$; $\gamma = 30$ degrees
Container C: $\alpha \cong 6.73$ degrees; $\beta = .22"/.44" = 0.5$; $\gamma \cong 28$ degrees

Figure 6 Nominal dimensions of constructed containers

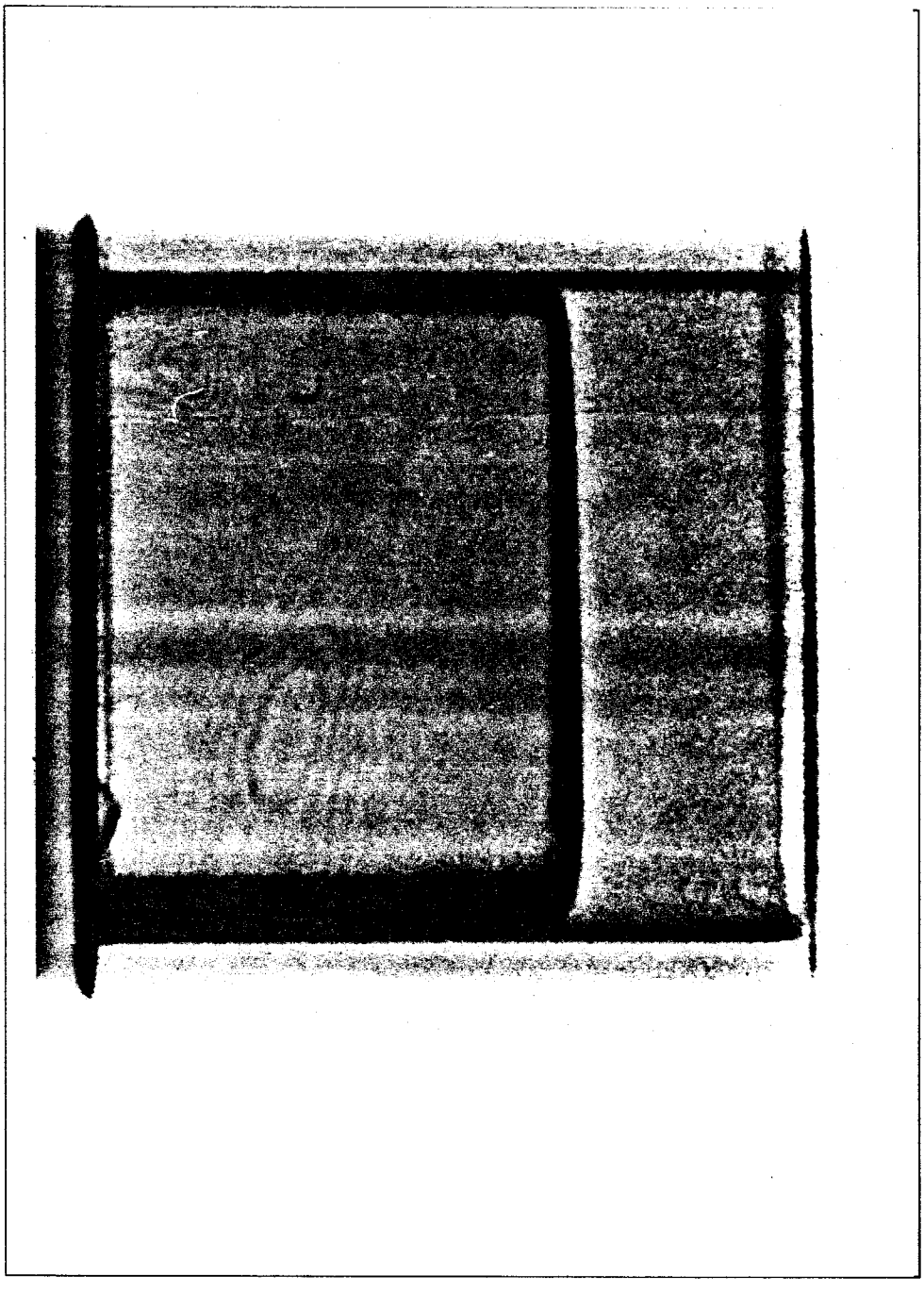

Figure 7a

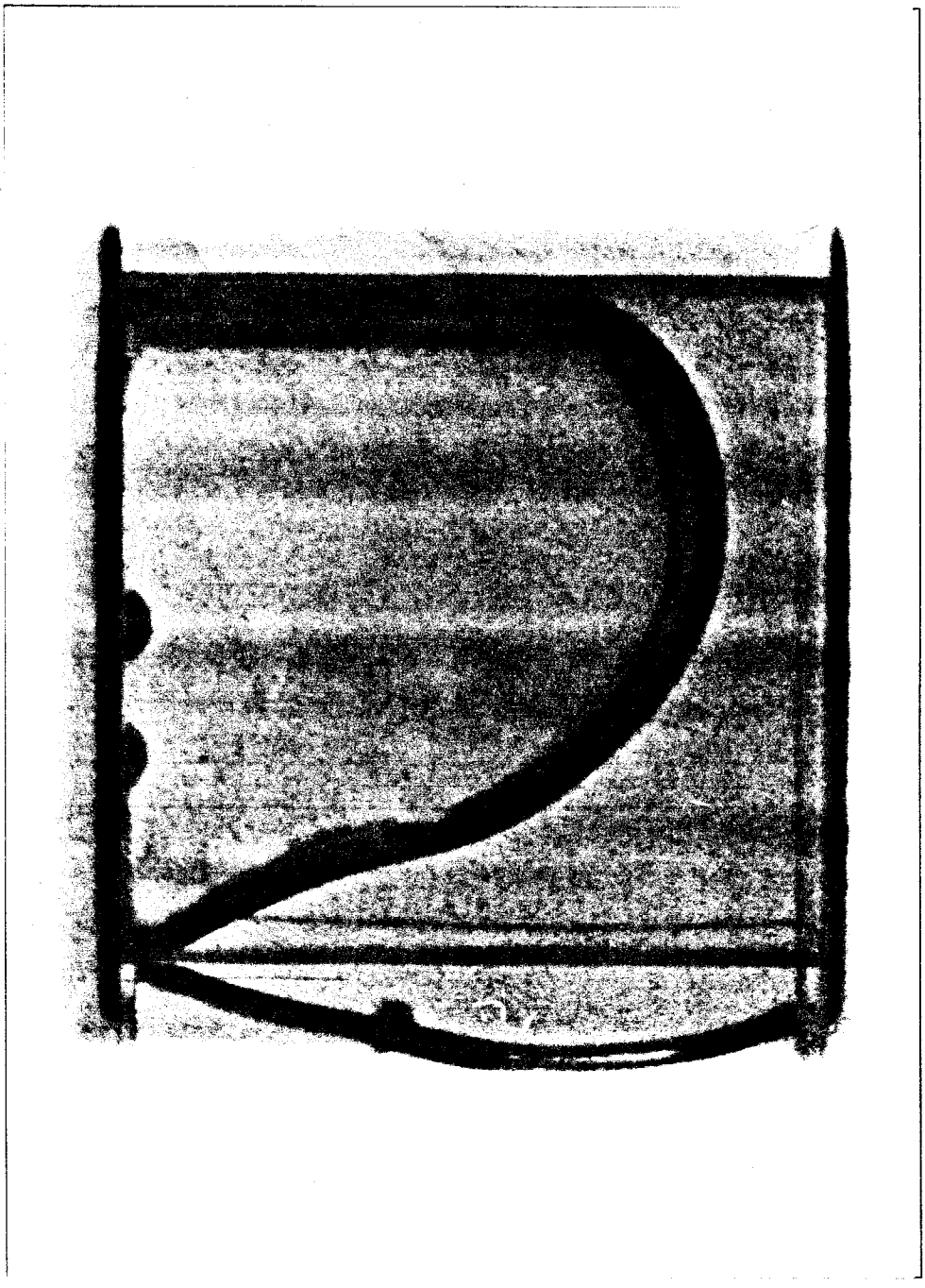

Figure 7b

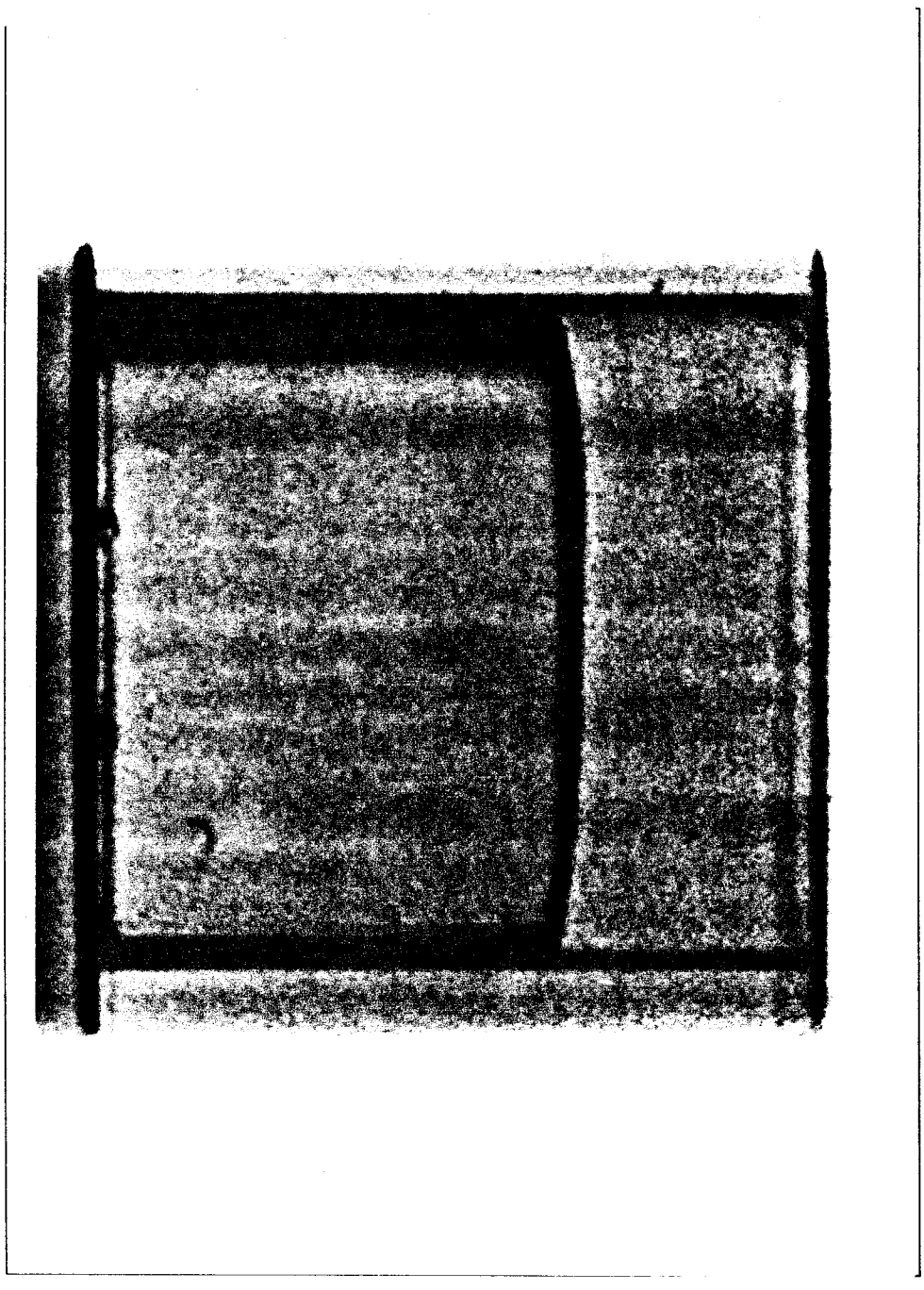

Figure 7c

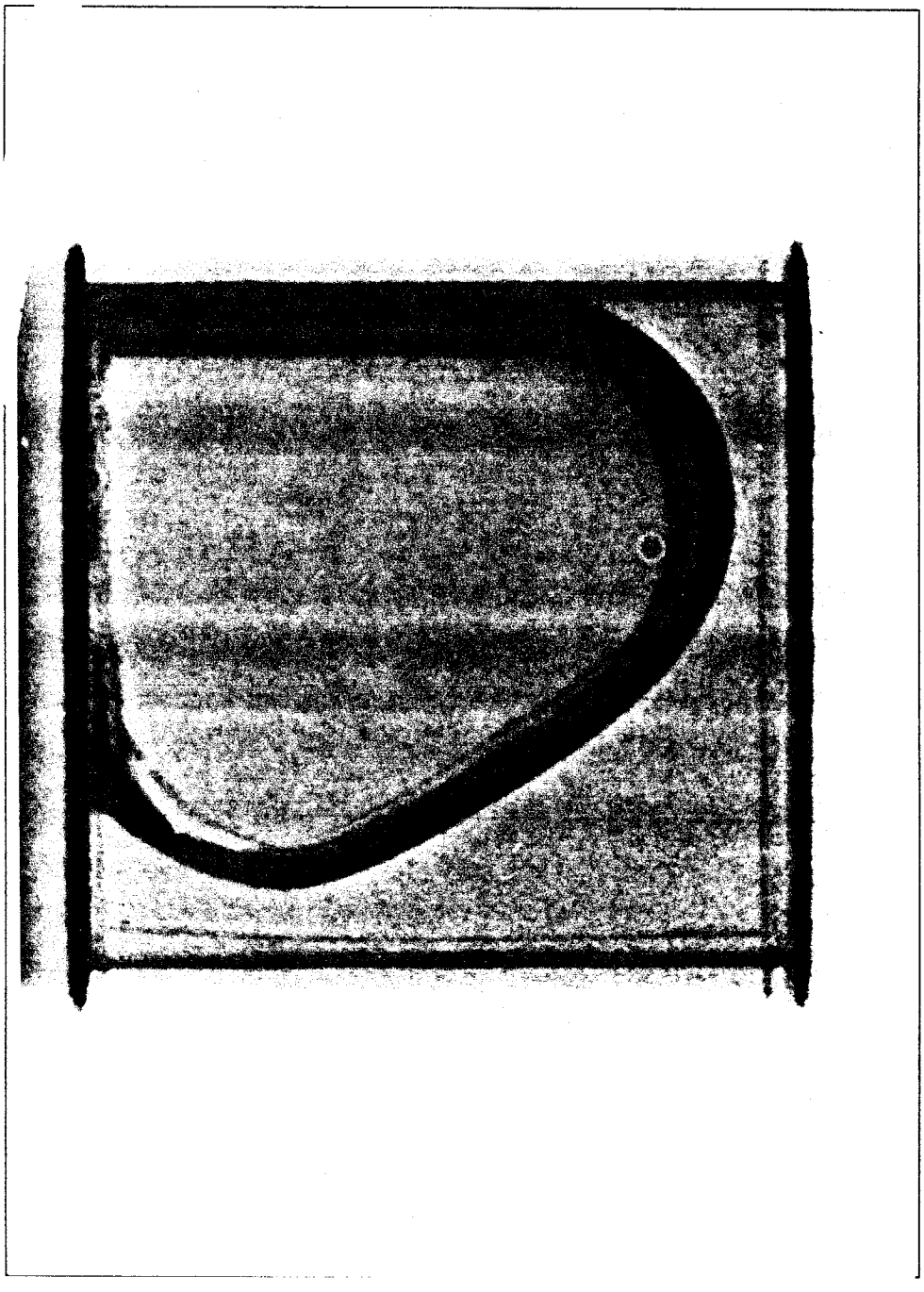

Figure 7d

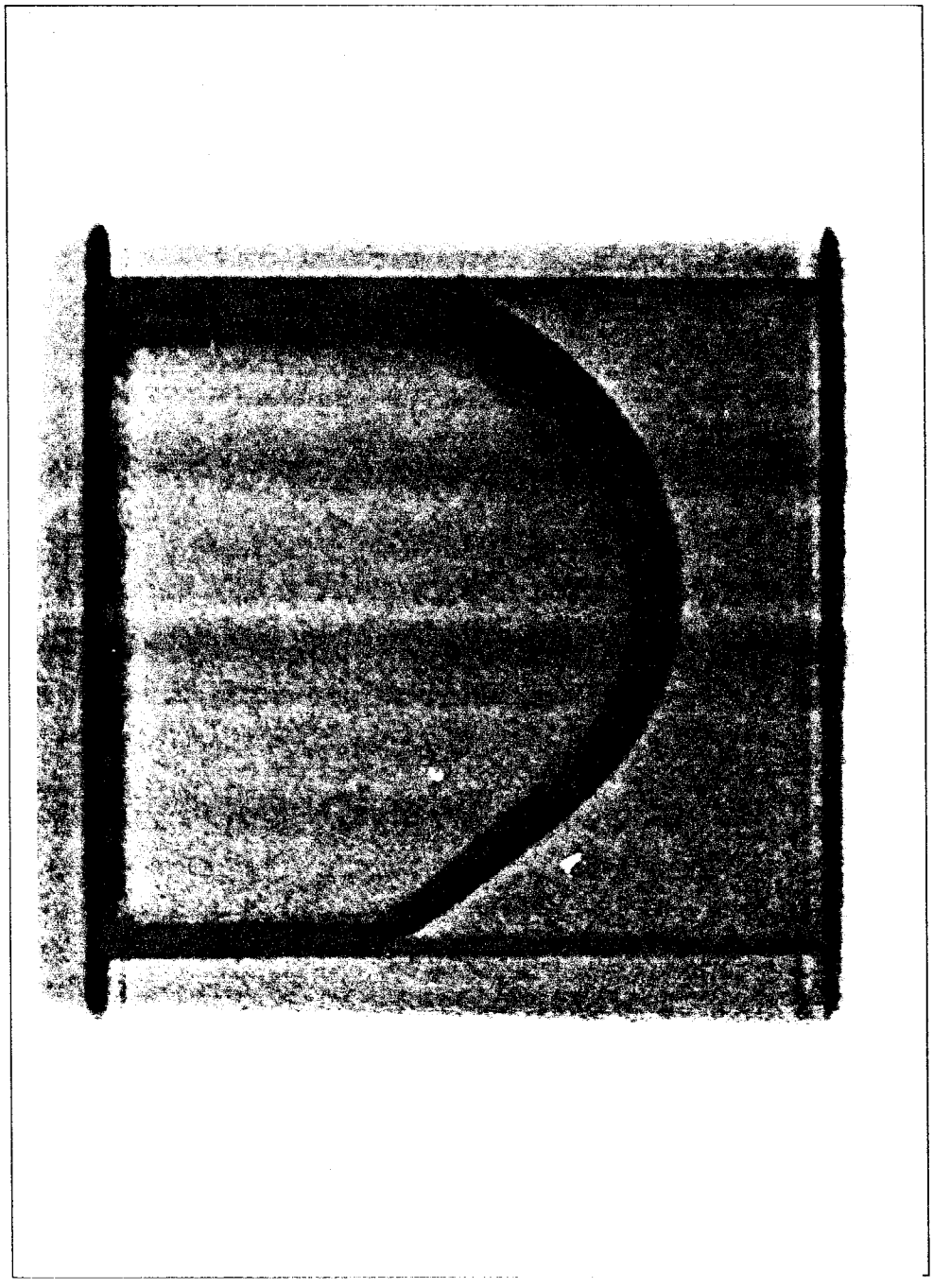

Figure 7e

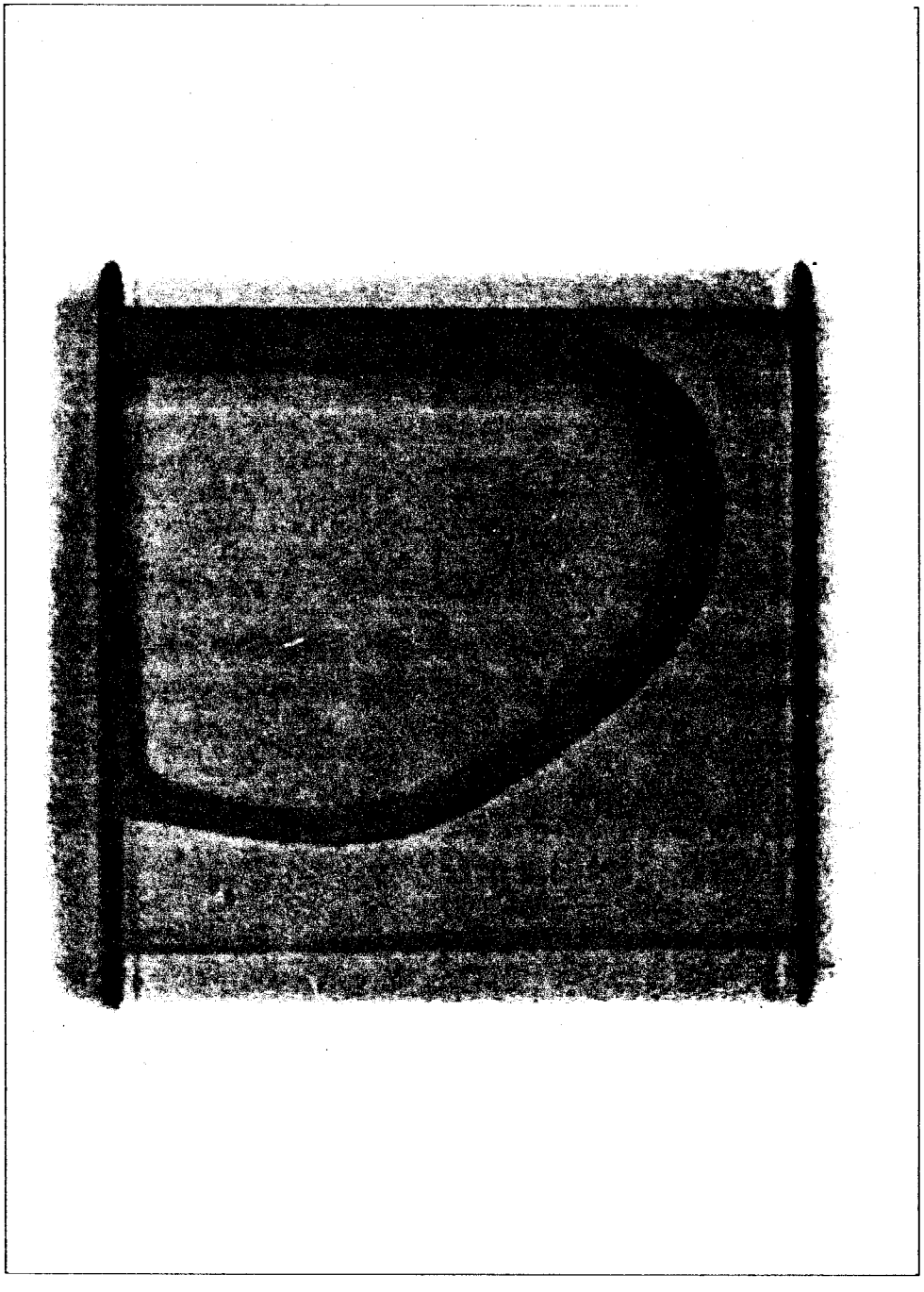

Figure 7f

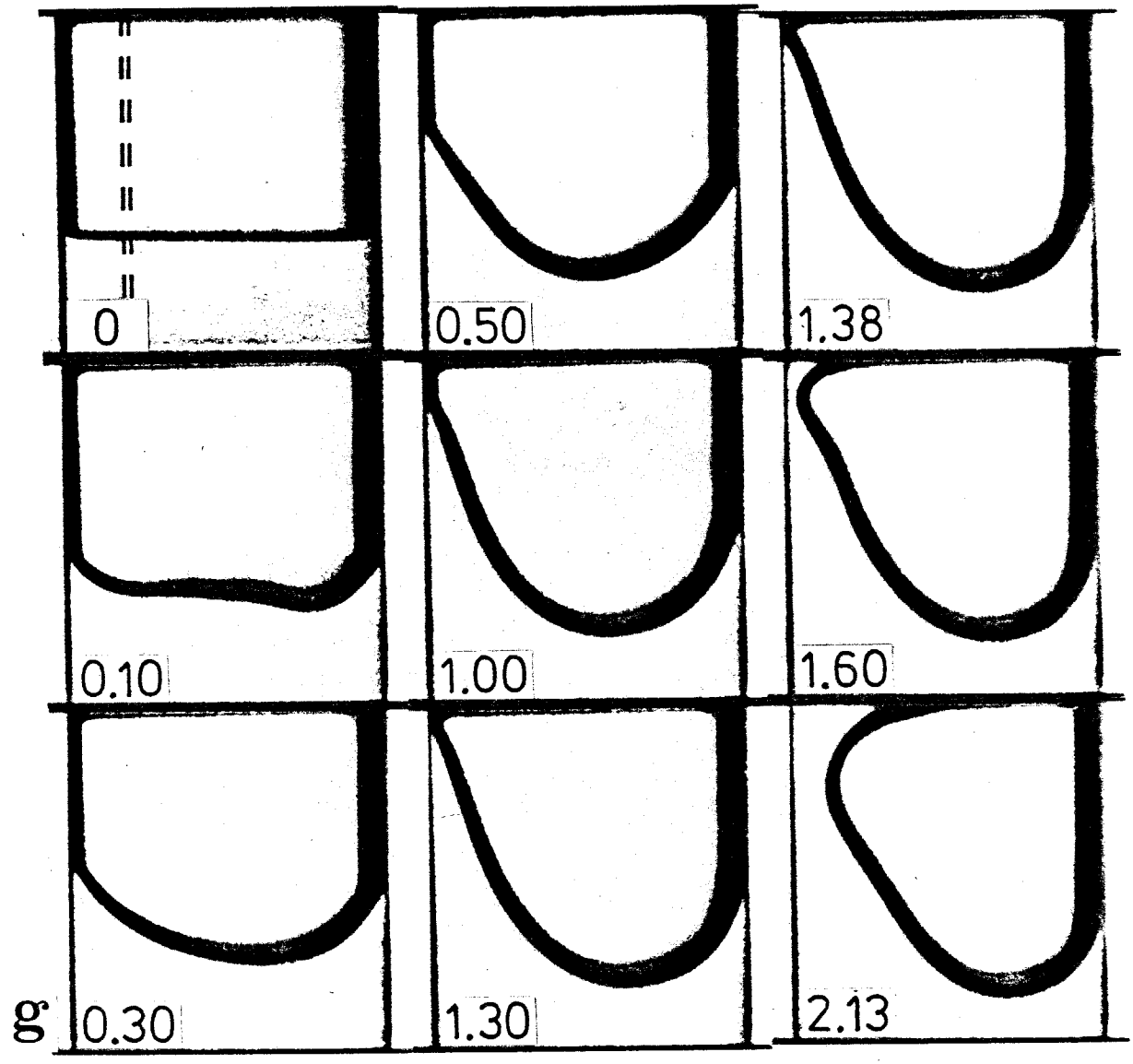

Figure 7g

Exp. Fluids 6U/2

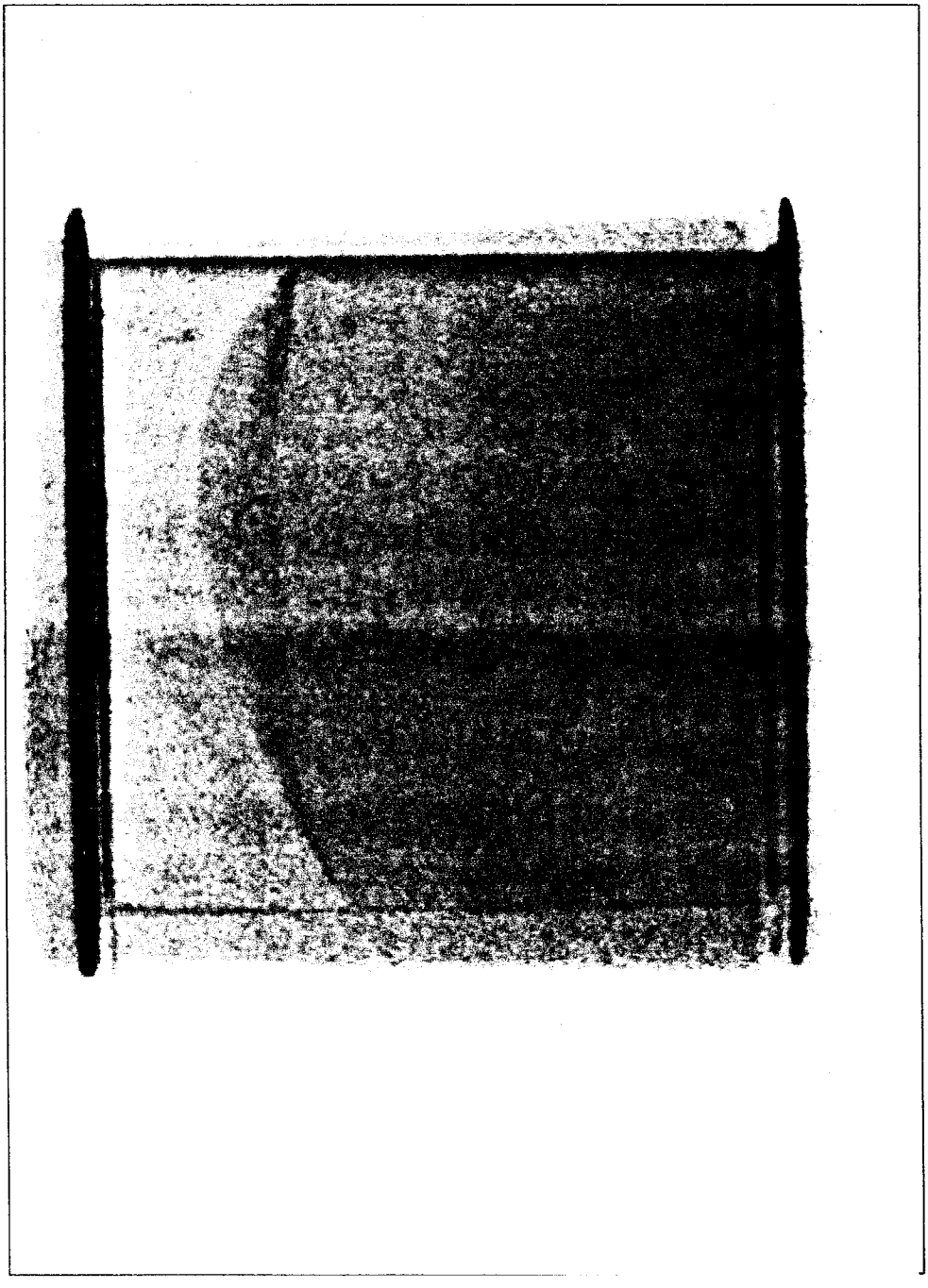

Figure 7h

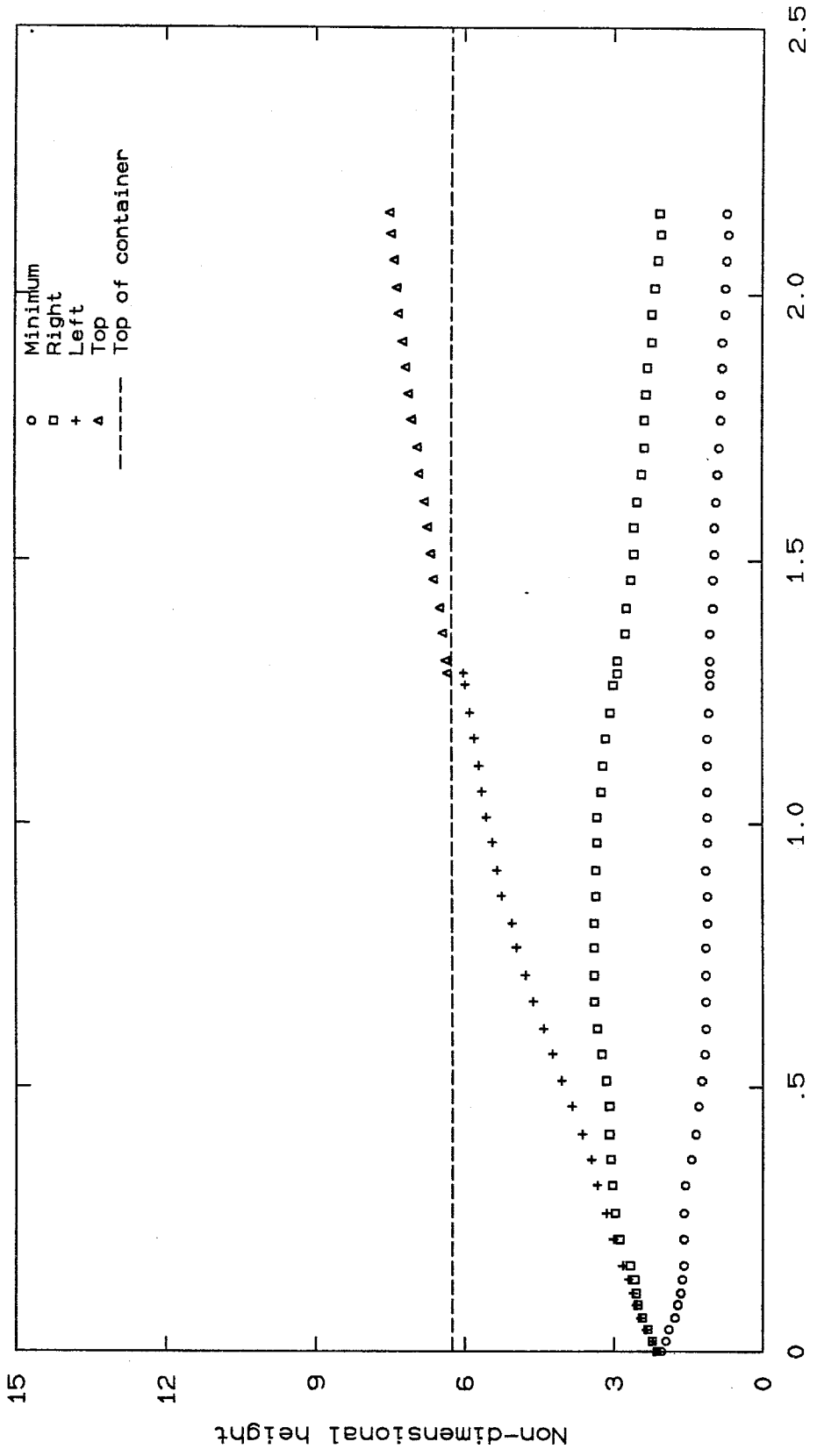

Figure 8a Position of free surface of 40 percent ethanol solution at zero gravity

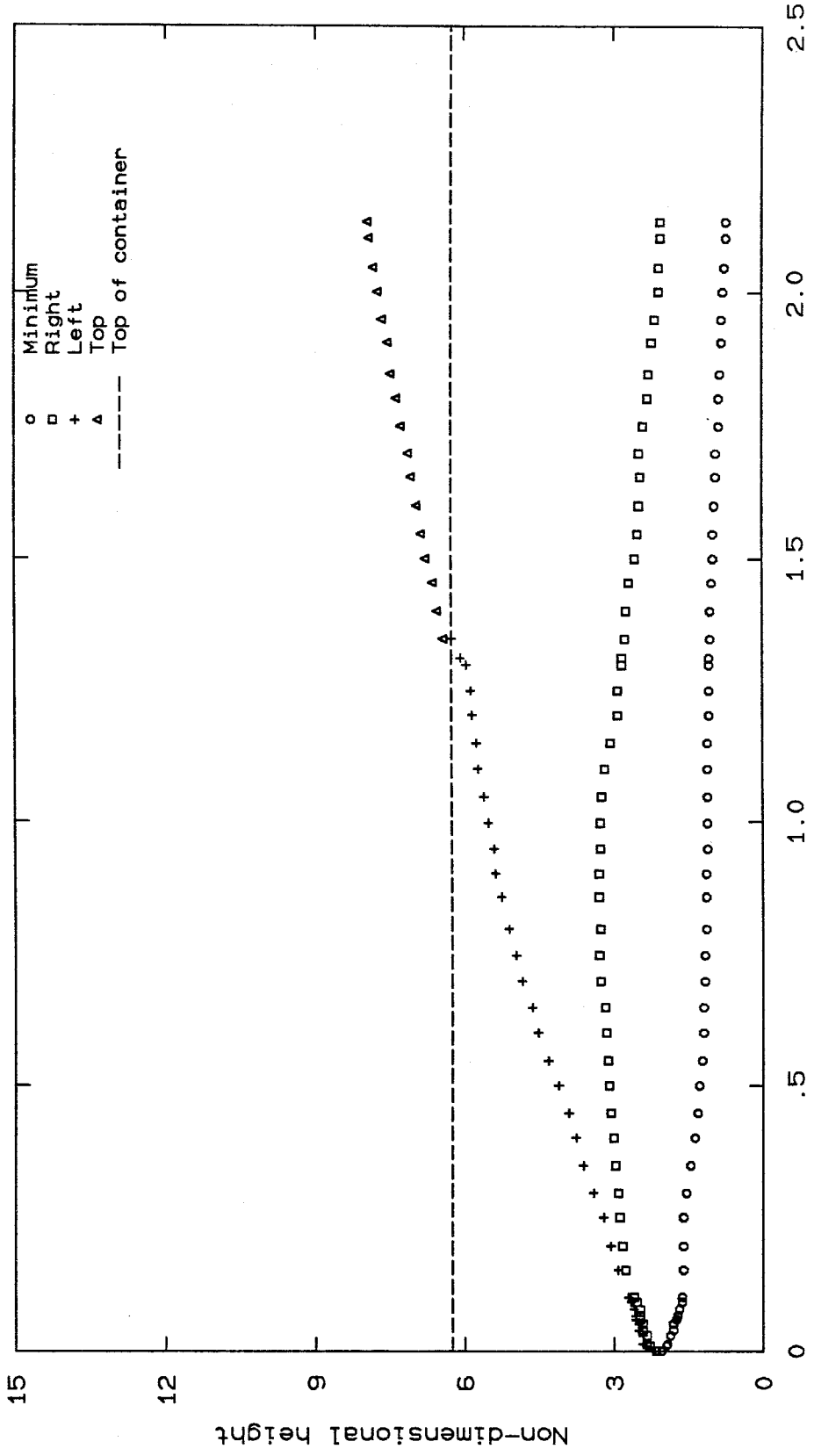

Figure 8b Position of free surface of 50 percent ethanol solution at zero gravity

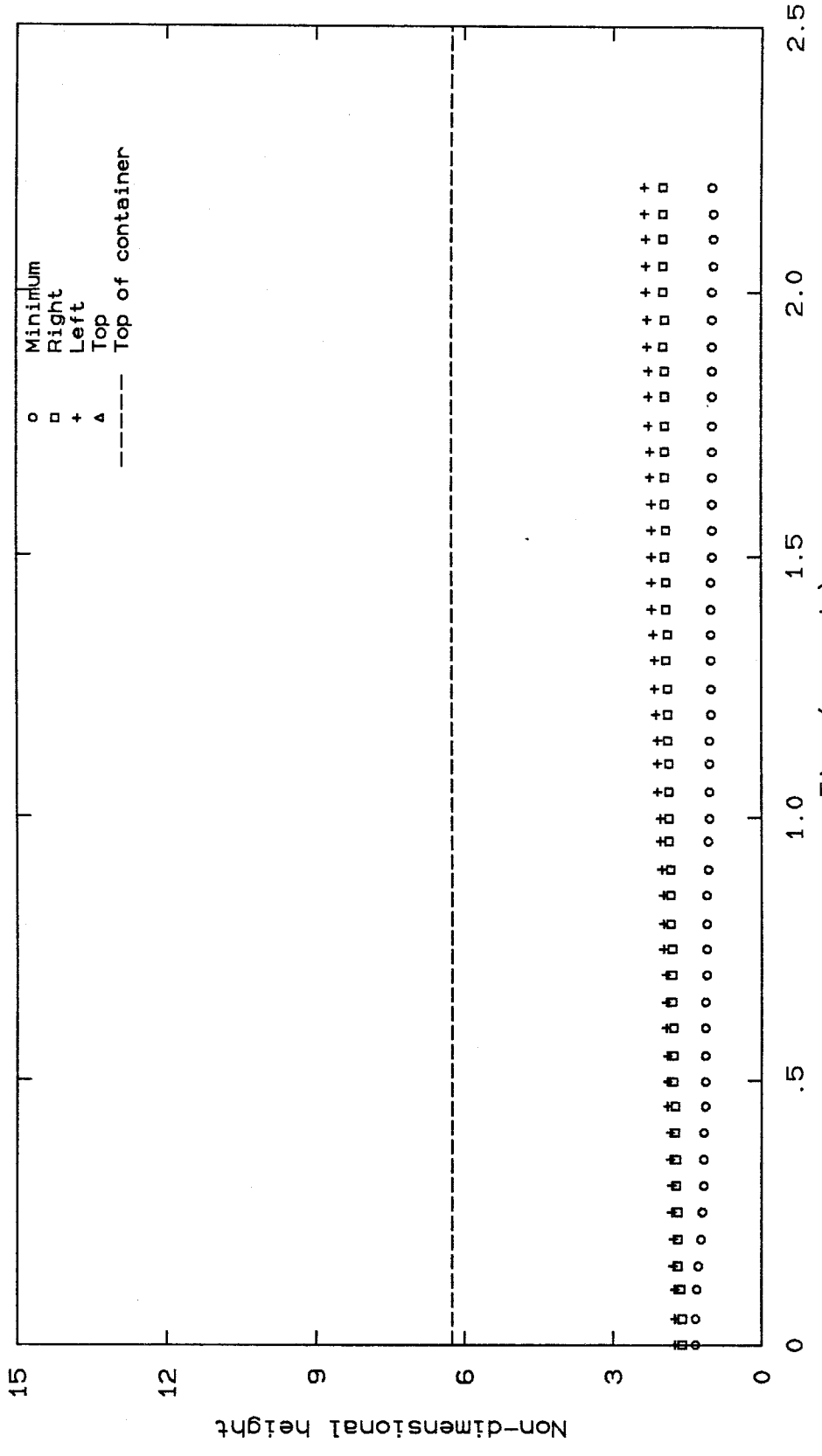

Figure 8c Position of free interface of glycerol tributanoate over ethylene glycol at zero gravity

Table 1: Liquid Pair Properties

Liquid Pair	Left Contact-Line Velocity ($\frac{cm}{sec}$)	σ $\left[\frac{dynes}{cm}\right]$	ρ (cP)	μ	γ	$\sigma \cos\gamma$
1	0.28	8.2	$\frac{1.035}{1.109}$	$\frac{11.6}{19.9}$	18°	7.80
2	0.09	7.1	$\frac{0.988}{1.133}$	$\frac{3.8}{4.5}$	29°	6.21
3	0.13	20.9	$\frac{0.879}{1.133}$	$\frac{0.8}{4.5}$	68°	7.83